Heterogeneous & Homogeneous & Bio- & Nano-
CHEMCATCHEM
CATALYSIS

Accepted Article

Title: Activated niobium and tantalum imido complexes: from tuneable polymerization to selective ethylene dimerization systems

Authors: Antonis Messinis, Andrei Batsanov, Judith Howard, Martin Hanton, and Philip William Dyer

To be cited as: *ChemCatChem* 10.1002/cctc.201801849

Link to VoR: http://dx.doi.org/10.1002/cctc.201801849

A Journal of
ChemPubSoc Europe

WILEY-VCH

www.chemcatchem.org

10.1002/cctc.201801849

WILEY-VCH

FULL PAPER

Activated niobium and tantalum imido complexes: from tuneable polymerization to selective ethylene dimerization systems

Antonis M. Messinis,[a],[b] Andrei S. Batsanov,[b] Judith A. K. Howard,[b] Martin J. Hanton,*[c],[d] and Philip W. Dyer *[a],[b]

Abstract: The niobium and tantalum imido complexes [CpMCl$_2$(NDipp)], [MCl$_3$(NR)(dme)] (R = *t*Bu, Ph, 2,6-*i*Pr$_2$C$_6$H$_3$ (Dipp), and Mes), and [TaCl$_3$(NDipp)(tmeda)] were tested in combination with EtAlCl$_2$ for the dimerization of ethylene. The niobium systems afforded dimers or polymers, depending on the nature of the imido ligand, with overall productivities in the range 720 to 13,720 (mol C_2H_4)(mol Nb)$^{-1}$. The nature of the polyethylene produced (LDPE or HDPE) depended on the imido ligand and the niobium concentration at which catalysis was run. In contrast, the tantalum/dme systems all mediated ethylene dimerization with productivities of up to 4,503 (mol C_2H_4)(mol Ta)$^{-1}$, with overall selectivities to butenes of between 73 - 81 wt%; selectivity within the dimer fraction to 1-butene was in the range 72 to 100%. The productivity of [TaCl$_3$(NDipp)(tmeda)] was six times higher than that of its dme-bearing counterpart, but at the cost of selectivity to 1-butene. For the tantalum imido-mediated ethylene dimerization the composition of the product slate formed is indicative of a metallacyclic mechanism being operative.

Introduction

The industrial importance of linear alpha olefins (LAOs) is well established. LAOs are used in the production of a wide range of everyday products such as synthetic lubricants, plasticizer and detergent alcohols, synthetic fatty acids, and polymers.[1] Consequently, the annual production of LAOs is significant at around 5 million metric tons, with a market worth of USD 14 billion in 2014.[1d] Of the various LAOs produced on an industrial scale, 1-butene is the most widely used, primarily as a co-monomer in the production of polyethylene,[2] but also in the production of methyl ethyl ketone and valeraldehyde, which are key intermediates used in the manufacture of flavours, perfumes, and pharmaceuticals.[3]

Due to the diverse, high-demand applications of LAOs, their efficient and economic manufacture is, and is likely to remain, an area of intense research. Indeed, to date a variety of ethylene dimerization and oligomerization systems have been developed employing mainly homogeneous, but also a limited number of heterogeneous catalysts,[4] which together encompass a range of metals including nickel,[5] cobalt,[6] iron,[6a] palladium,[7] platinum,[8] chromium,[9] molybdenum,[10] and vanadium.[11] Currently, the most industrially relevant ethylene dimerization system is that employed in Axens' AlphaButol process. This comprises a soluble catalyst derived from [Ti(O^{i}Pr)$_4$]/triethylaluminium, operating at 50-55 °C and 20-27 bar ethylene pressure.[12] The dimerization activities obtained in the AlphaButol process are moderate, lying in the range 170 to 16,550 (mol C_2H_4)(mol Ti)$^{-1}$h^{-1}. Nevertheless, the lack of high catalytic activity is offset by the high selectivity of the AlphaButol system towards 1-butene (93-95%), which is accompanied by only low levels of polymer formation (<0.5 wt%),[12a, 12c-j] a factor that is significant since it helps minimize reactor fouling and maximises atom economy.[13]

Following our study of the olefin dimerization performance of various molybdenum imido-derived catalytic systems,[10] we reported recently the use of a series of analogous tungsten imido pre-catalysts for the conversion of ethylene to 1-butene. Compared to their lighter group 6 congeners these tungsten systems display much higher activity (up to 409,410 (mol C_2H_4)(mol W)$^{-1}$h^{-1}) and selectivity (up to 85.5 wt% in 1-butene).[14]

With these results in hand, we wanted to explore if this periodic performance trend was evident for other transition metal imido dimerization catalyst systems. In this context, Nomura and co-workers have extensively described the application of vanadium imido pre-catalysts.[11] However, to the best of our knowledge, there are no reports of niobium-containing dimerization catalysts, and only scarce examples of tantalum-based systems.[15] Given that versatile syntheses of both niobium and tantalum imido complexes are well established,[16] herein we explore the applicability of such niobium and tantalum imido complexes in catalytic ethylene dimerization in combination with EtAlCl$_2$. In particular, the influence of the readily varied organoimido substituent is explored.

Results and Discussion

Synthesis and characterization of complexes

[a] Dr Antonis M. Messinis and Dr Philip W. Dyer
Center for Sustainable Chemical Processes,
Department of Chemistry
Durham University
South Road, Durham, DH1 3LE, UK
E-mail: p.w.dyer@durham.ac.uk
[b] Dr Andrei S. Batsanov, Prof. Judith A. K. Howard
Department of Chemistry
Durham University
South Road, Durham, DH1 3LE, UK
[c] Dr Martin J. Hanton
Sasol UK Ltd
Purdie Building, North Haugh, St Andrews, Fife, KY16 9ST, U.K.
[d] Current address: TÜV SÜD Ltd, East Kilbride, Glasgow, G75 0QF, UK
E-mail: Martin.Hanton@tuv-sud.co.uk
Supporting information for this article is given via a link at the end of the document.

The niobium and tantalum imido complexes **1**-**4** were synthesized according to literature procedures (or adaptations thereof) from the respective pentahalides (Scheme 1).[16] Previously unreported complexes **2c** and **4c** were structurally characterized by single-crystal X-ray diffraction (Figure 1), together with **2b**, **4a** and two polymorphs of **4b** (see SI).[16a]

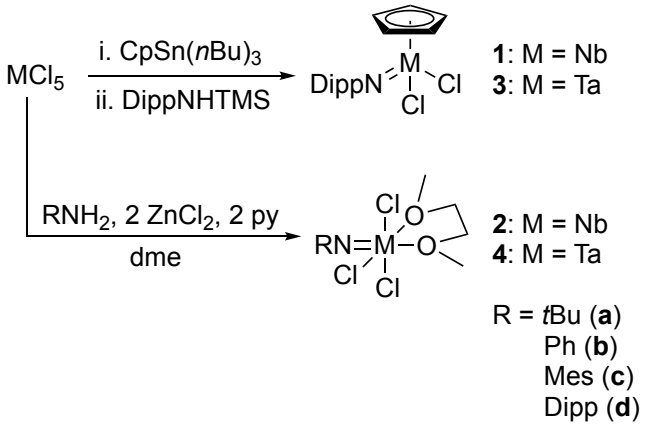

Scheme 1. Synthesis of niobium and tantalum imido complexes **1**–**4**, using previously reported procedures or modifications thereof.[16]

The complexes **2a-d** and **4a-d** (Tables S5, S6) were found to all have distorted octahedral coordination about the metal atom, with a *mer* arrangement of the Cl ligands. Quantitatively, the distortion was described by the displacement of the metal atom from the Cl(1)Cl(2)Cl(3)O(2) plane towards the N atom (0.33-0.38 Å), Table 1. The metal-nitrogen distances are all typical of *pseudo* triple bonds, lying between 1.72 and 1.77 Å.[17] The shortest M-N distances were found for the *t*Bu imido complexes **2a** (1.722(2) Å) and **4a** (1.747(3) Å), with those of the aryl-substituted derivatives being longer due to conjugation between the aromatic ring and M≡N π-systems (evidenced by short N-C bonds).

In assessing the catalytic dimerization performance of the various imido complexes we have tested here, we sought to establish a correlation with the steric and electronic characteristics of the various organoimido (NR) motifs. The steric demands of each of the imido substituents was assessed using the percentage buried volume (%V_{Bur}) and topographic steric map approaches approach developed by Cavallo and co-workers.[18] This methodology imbeds the ligand of interest within a sphere of set radius from the metal centre. From the van der Waals radius of each atom within this sphere, the percentage volume occupied by the ligand (%V_{Bur}) was calculated from the experimentally-determined X-ray crystallographic data using the free online software, SambVca.[19] The parameters used to calculate the %V_{Bur} for the various organoimido fragments using SambVca are described in the SI.

The %V_{Bur} analysis revealed the steric demands of the various imido substituents to lie in the order NPh < *t*BuN < NMes < NDipp for both series of complexes **2a-d** and **4a-d**, albeit with only modest differences (Table 1). However, it must be noted that the %V_{Bur} values calculated for the NDipp imido complexes **2d** and **4d** are likely to be underestimated (especially when compared to the clearly less bulky NMes group in complexes **2c** and **4c**) due to the lack of symmetry of the Dipp moiety, which results in the isopropyl methyl groups being located away from the metal in the solid state molecular structures used to calculate %V_{Bur}. In solution, rotation of the Dipp motif will result in increased steric demands around the metal centre. Analysis of the computed topographic steric maps (Table S1),[18a] indicated that the organoimido substituents R are remote from the metal centre (negative scale in the steric maps, Figure S14). Consequently, the direct steric pressure of the imido ligands on the other ligands bound at the metal will be minimal, although the organic substituents clearly occupy different regions of space within the metals' wider coordination sphere.

Table 1. Analysis of the steric impact of organoimido ligands in complexes **2a-d** and **4a-d** using the %V_{Bur} approach, estimation of the *trans* influence, Δd_{MO}, and the degree of distortion away from true octahedral geometry, δ(M).

Complex	%V_{Bur} [a]	δ(M), Å [b]	Δd_{MO}, Å [d]	Ref.
[$NbCl_3$(N*t*Bu)(dme)] (**2a**)	18.7	0.329 [c]	0.202(8)	[5]
[$NbCl_3$(NPh)(dme)] (**2b**)	17.0	0.327	0.132(2)	this work
[$NbCl_3$(NMes)(dme)] (**2c**)	21.1	0.325 [c]	0.153(2) [c]	this work
[$NbCl_3$(NDipp)(dme)] (**2d**)	21.8	0.328	0.120(5)	[6]
[$TaCl_3$(N*t*Bu)(dme)] (**4a**)	19.1	0.375	0.222(3)	this work
[$TaCl_3$(NPh)(dme)] (**4b**)	16.8	0.335 [c]	0.160(5) [c]	this work
[$TaCl_3$(NMes)(dme)] (**4c**)	21.0	0.347	0.191(6)	this work
[$TaCl_3$(NDipp)(dme)] (**4d**)	21.6	0.340	0.128(8)	[6]

[a] Values calculated using the SambVca software [19] and the parameters defined in the SI. [b] Displacement of the M atom towards N from the plane of four *cis*-ligands, L_{cis} = Cl(1), Cl(2), Cl(3) and O(2) in the present work. [c] Average of independent molecules. [d] degree of lengthening (Δd_{MO}) of the *trans* M-O(1) *versus* the *cis* M-O(2) bonds (Tables S5, S6).

The relative differences in the *trans* influence of a wide range of ligands, including imido groups, have been used extensively to assess ligand electronic and, to an extent, steric demands.[17, 20] Consequently, the *trans* influence of the imido motifs in the two series of structurally analogous complexes **2a-d** and **4a-d** were assessed. Given the deviation from ideal octahedral geometry for these *mer*-[MCl_3(NR)(dme)] complexes, in particular the deviation from linearity of the *trans*-N-M-O bond angle (~167-171°), the *trans* influences were estimated from the degree of lengthening (Δd_{MO}) of the *trans* M-O(1) *versus* the *cis* M-O(2) bonds (Tables S5, S6). The statistically significant values of Δd_{MO} for both the niobium (**2a-d**) and tantalum (**4a-d**) complexes vary from 0.12 to 0.22 Å, with values for both series increasing in the order NDipp < NPh < NMes < N*t*Bu. This experimentally-determined *trans* influence ordering exactly parallels the electronic characteristics of the four different organoimido motifs as assessed from the pK_a values of the parent aminimum ions (RNH_3^+): R = Dipp (4.38), Ph (4.64), Mes (4.65), and *t*Bu (10.71).[21] Although it has been reported previously that the origins of the *trans* influence of imido ligands in an octahedral coordination manifold are complex (including π-electronic effects and electronic repulsion),[22] our observations are consistent with electronic factors being the principal component contributing to

the variation in *trans* influence of imido ligands of complexes **2a-d** and **4a-d**.[23]

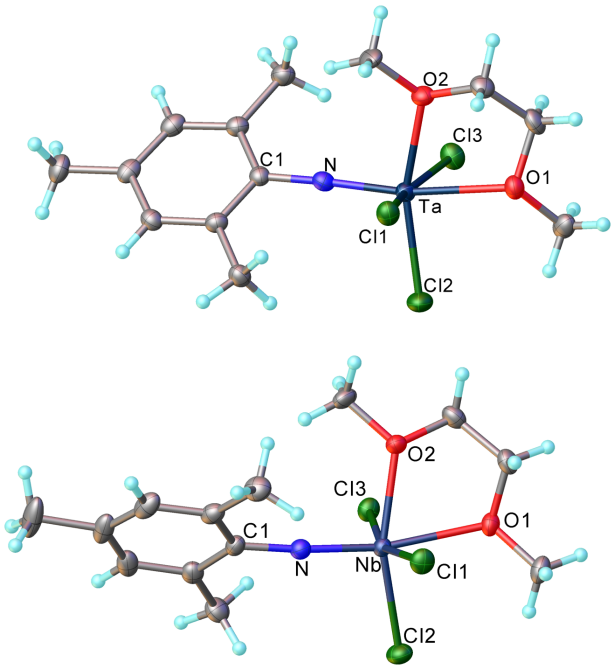

Figure 1. X-Ray molecular structures of [$NbCl_3$(NMes)(dme)] (**2c**, top, one of the independent molecules) and [$TaCl_3$(NMes)(dme)] (**4c**). Thermal ellipsoids are shown at the 50% probability level.

Catalyst testing

The catalytic ethylene oligomerization performance of the niobium and tantalum complexes **1** to **4** was screened using 15 equivalents of $EtAlCl_2$ as activator at 60 °C, 40 barg ethylene pressure, and with chlorobenzene as solvent (Table 2). The reaction conditions employed here mirror those previously optimised for related industrially-competitive tungsten imido-based dimerization systems, thus allowing direct comparison of the performance of the Nb and Ta imido complexes.[10, 14, 24] Utilisation of chlorobenzene as reaction medium for the catalytic testing was adopted since we have previously demonstrated that this was the optimal solvent for ethylene dimerisation mediated by tungsten imido pre-catalysts and hence its choice facilitates a direct comparison of the performance of the group 5 and 6 catalyst systems; note, catalyst optimisation was not a focus of this current study.[14, 24] Use of $EtAlCl_2$ rather than less well-defined aluminoxane-type activators (*e.g.* MAO or MMAO) was chosen to avoid differences in performance arising from well-documented batch-to-batch variations for the latter.[25] Each

Table 2. Results from catalytic ethylene dimerization tests conducted at 40 barg ethylene pressure and 60 °C with niobium (**1**, **2a-d**) and tantalum (**3**, **4a-d**) complexes and $EtAlCl_2$ as activator.[a]

Run #	Pre-catalyst	Time, min	TON[b]	Activity[c]	Product mass, g	PE, wt%	Selectivity within the liquid fraction[d, e]				
							C_4, wt% (1-C_4 in C_4, %)	1-C_4, wt%	C_6, wt% (1-C_6 in C_6, %)	Linear C_6 in C_6, %	C_{8+}, wt%
1	[$CpNbCl_2$(NDipp)] (**1**)	10	720	4,340	0.406	1.1	97.9 (97.9)	95.8	2.1 (0.00)	-	0.0
2	[$NbCl_3$(N*t*Bu)(dme)] (**2a**)	3.4	4,600	81,190	2.581	62.7	75.8 (97.8)	74.1	7.4 (100)	92.8	16.8
3	[$NbCl_3$(NPh)(dme)] (**2b**)	7.5	8,600	68,610	4.825	5.2	92.9 (85.6)	79.5	6.2 (35.6)	85.1	0.9
4	[$NbCl_3$(NMes)(dme)] (**2c**)	2.3	2,290	59,830	1.287	25.1	93.5 (94.7)	88.5	4.4 (69.6)	90.7	2.1
5	[$NbCl_3$(NDipp)(dme)] (**2d**)	7.9	13,720	104,200	7.698	70.7	8.8 (98.6)	8.7	4.2 (92.0)	85.0	87.0
6	[$NbCl_3$(NDipp)(dme)] (**2d**) [f]	7.8	9,450	72,380	1.325	60.2	62.7 (98.0)	61.4	5.3 (88.1)	100.0	32.0
7	[$CpTaCl_3$(NDipp)] (**3**)	10	300	1,790	0.167	6.0	73.0 (100)	73.0	15.4 (74.0)	85.1	11.6
8	[$TaCl_3$(N*t*Bu)(dme)] (**4a**)	6.5	3,780	34,970	2.123	2.7	79.8 (100)	79.8	19.3 (67.4)	72.4	0.9
9	[$TaCl_3$(NPh)(dme)] (**4b**)	5.6	2,800	29,940	1.573	2.2	80.7 (100)	80.7	17.9 (77.8)	81.7	1.4
10	[$TaCl_3$(NMes)(dme)] (**4c**)	5	2,410	28,590	1.349	7.0	77.6 (99.8)	77.4	21.2 (75.6)	80.7	1.2
11	[$TaCl_3$(NDipp)(dme)] (**4d**)	7.6	4,500	35,710	2.527	8.8	79.3 (100)	79.3	17.2 (64.1)	68.9	3.5
12	[$TaCl_3$(NDipp)(tmeda)] (**5**)	75	26,450	21,160	14.839	0.0	79.6 (72.4)	57.6	15.1 (33.2)	79.5	5.3

[a] Conditions: 20 µmol metal complex; 300 µmol $EtAlCl_2$; PhCl 74 mL; 60 °C; ethylene pressure (40 barg); stirrer speed 1000 rpm; nonane standard (1.000 mL); catalytic runs were performed until consumption of C_2H_4 dropped below 0.2 g min^{-1} or until the reactor was filled. [b] TON (productivity) is reported in (mol C_2H_4)(mol M)$^{-1}$. [c] Activity is reported in (mol C_2H_4)(mol M)$^{-1}$ h^{-1}. [d] Selectivity to dimers, trimers, and oligomers within the total soluble product fraction expressed in wt%. The % content of the linear terminal olefin within the dimer and trimer fractions are in parentheses. [e] Investigation of catalytic reproducibility and error analyses are detailed in Ref. [14b]. [f] 5.0 µmol of complex and 75.0 µmol of $EtAlCl_2$ were used.

catalyst test was allowed to run until ethylene uptake dropped below the detection limit (0.2 g min^{-1}), to gain information on the lifetime of the catalytic system. Only reporting activities can be misleading in terms of overall catalytic performance, with very high activities being achieved by stopping the reaction just after the most productive phase of catalysis.

Ethylene dimerization with niobium imido complexes

The organic products produced using each of the niobium pre-catalysts **1**,**2a-d** were polyethylene, butenes, and small amounts of hexenes in ratios heavily dependent on the metal's substitution pattern (Table 2, Runs 1-6). Nevertheless, the selectivity towards 1-butene within the C_4 fraction was high in all cases, ranging between 85.6% and 98.6%, indicating that little 1-butene isomerization occurred during catalysis. Complex **1** exhibited the lowest activity and productivity within the series of niobium imido complexes screened, 4,342 (mol C_2H_4)(mol Nb)$^{-1}$ h^{-1} and 724 (mol C_2H_4)(mol Nb)$^{-1}$, respectively (Run 1). Like complex **1**, the structurally similar complex [$CpNbCl_2$(N-2-*t*Bu-C_6H_4)] was also a poor ethylene polymerization catalyst when activated with 30 equivalents of Et_2AlCl.[26] Similar low polymerization activity was seen with other CpNb-based catalysts.[15f, 27] Consideration of the computed topographic steric maps for complexes **1** and **2d** (Table S1) very clearly demonstrated the geometric and steric constraints imposed on the incoming substrate olefin for **1** consistent with its low activity. The poor activity achieved using pre-catalyst **1** is consistent with its high selectivity towards 1-butene; the low concentration of 1-butene present limited re-incorporation/oligomerization.[28] Although steric constraints are likely to significantly influence the catalytic performance of **1**, electronic effects from the Cp ligand cannot however be excluded.

The catalytic behaviour of pre-catalysts **2** was dependent on the nature of the imido substituent: **2b** produced mainly butenes (Table 2, Run 3), **2a** and **2d** showed selectivity to polymer over butenes, (Table 2 Runs 2 and 5), while **2c** covered the middle ground between dimerization and polymerization with 25.1 wt% of the products comprising polyethylene (Table 2, Run 4). The polymerization activities observed with pre-catalysts **2** were comparable to those of previously reported niobium-based ethylene polymerization systems.[27, 29]

For pre-catalysts **2b-d** (Figure 2) as the steric demands of the imido substituents were increased (NPh < NMes < NDipp; see Table 1), so the extent of oligomer (>C_4) and polymer formation increased (Figure 2). This trend is attributed mainly to steric effects since not only are the structures of complexes **2b-d** identical (*vide supra*), but the electronic characteristics of the NDipp, NMes, and NPh groups can be regarded as near-equivalent based on the pK_a values (in water) of the corresponding anilines ($PhNH_2$, $MesNH_2$, and $DippNH_2$), which lie in the range 4.0 and 4.6.[21] In contrast, although the organoimido moiety of the pre-catalyst [$NbCl_3$(N*t*Bu)(dme)] (**2a**) occupies a slightly greater volume than that of the imido unit in the phenylimido derivative **2b**, $\%V_{Bur}$ = 18.7 (*t*Bu) and 17.0 (Ph), something that might be anticipated to favour polymerization (*vide infra*), the *t*BuN moiety (pK_a $tBuNH_2$ = 10.7) is significantly more electron-rich than the PhN unit and hence the origins of the product selectivity could not be attributed definitively (*c.f.* Runs 2 and 3).

Since the niobium complex **2d** afforded significant amounts of polyethylene, something that has a direct impact on the viscosity of the reaction medium, the influence of mass transfer effects on the organic product distribution was probed by repeating the test described in Run 5 (Table 2) at a higher dilution (Run 6). This reduction in niobium concentration led to a decrease in the overall catalytic activity and productivity (TON) from 104,199 to 72,375 (mol C_2H_4)(mol Nb)$^{-1}$ h^{-1} and 13,720 to 9,449 (mol C_2H_4)(mol Nb)$^{-1}$, respectively, instead of the anticipated increase due to the improved mass transfer of ethylene. This drop in performance in Run 6 was accompanied by a slight decrease in the selectivity towards polyethylene (from 70.7 to 60.2 wt%), while the amount of butene within the liquid fraction dramatically increased from 8.7 to 61.4 wt% at the expense of C_{8+} oligomers.

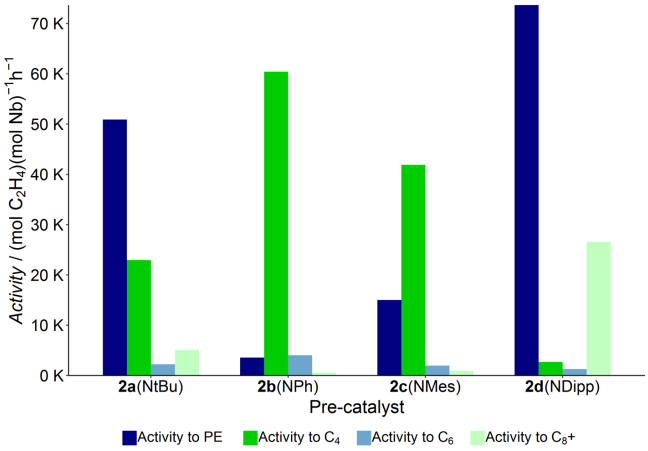

Figure 2. Comparison of catalytic activity towards polyethylene, butenes, hexenes, and oligomers as a function of organoimido ligand substituent of the niobium pre-catalysts **2a-d**.

The properties of the insoluble polyethylenes produced using each of the pre-catalysts/conditions were probed by DSC (Differential Scanning Calorimetry) analysis (Table S2). The materials isolated from each of the Runs 2-4 (pre-catalysts **2a-c**) were characteristic of HDPE.[30] In contrast, the nature of the polyethylene produced using complex **2d** (Table S2, Run 5) was consistent with it being a blend of HDPE rich in LDPE.[31] However, when the catalysis test was repeated at a lower concentration of complex **2d** (Table 2, Run 6) HDPE is produced with the highest peak melting temperature, density, and crystallinity observed within the series (Table S2). Thus, the catalytic behaviour of the Nb imido complexes **2a-d** with $EtAlCl_2$ as activator can be tuned not only in terms of the product selectivity (1-butene versus polyethylene), but also in terms of the nature of the polyethylene produced.

From a mechanistic perspective it is not possible for a single catalytically-active species to simultaneously selectively produce dimers and polymers under the same operating conditions (*e.g.* **2c**). Consequently, the variations in product distributions achieved using pre-catalysts **2a-d** were attributed to the formation of dimerization-, oligomerization-, and polymerization-active species in ratios that are governed by the nature of the

organoimido substituent. This helps explain the decreased formation of LDPE, which occured on lowering the pre-catalyst **2d**/15 $EtAlCl_2$ concentration (Table 2, Runs 5 and 6). It is speculated that the ethylene polymerization catalyst formed during Run 5 is able to co-polymerize ethylene with the 1-butene and oligomers produced *in situ* from the ethylene oligomerization catalyst that forms simultaneously upon activation (Scheme 2, top). This type of *in situ* co-polymerization (also known as concurrent tandem catalysis) is well documented.[32] At a lower niobium concentration (Table 2, Run 6) less active oligomerization and polymerization catalysts (lower overall catalytic activity) were formed, which being less capable of incorporating α-olefins lead to selective formation of 1-butene and HDPE (low levels of branching), respectively (Scheme 2, bottom). Note, the differences in composition of the polymeric materials produced using **2d** at different concentrations could also be attributed to chain walking at higher concentration, leading to formation of the observed LDPE. Although this would be consistent with a number of reports in which late transition metal-based polymerisation catalysts have been shown to afford LDPE *via* such a chain walking mechanism (Scheme 3), very few examples of such behaviour are known for early transition metal systems and is hence unlikely here.[33, 34] Furthermore, the niobium systems **2** also gave reasonable selectivity to 1-butene and linear hexenes (*e.g.* 35.6% 1-hexene selectivity, Table 1, entry 3), whose formation is at odds with chain walking. To help discriminate between a co-polymerisation or a chain walking pathway, or indeed the possibility that both types of mechanism were operative, the structure of the resulting LDPE should be studied by $^{1}H/^{13}C$ NMR spectroscopy. If the LDPE product only contains ethyl and butyl branches, a chain walking mechanism can be eliminated.[33, 34] However, attempts to undertake spectroscopic analysis of the polymeric materials obtained was precluded by their incomplete solubility in either 1,1,2,2-tetrachlorethane (TCE) or trichlorobenzene even at elevated temperatures.

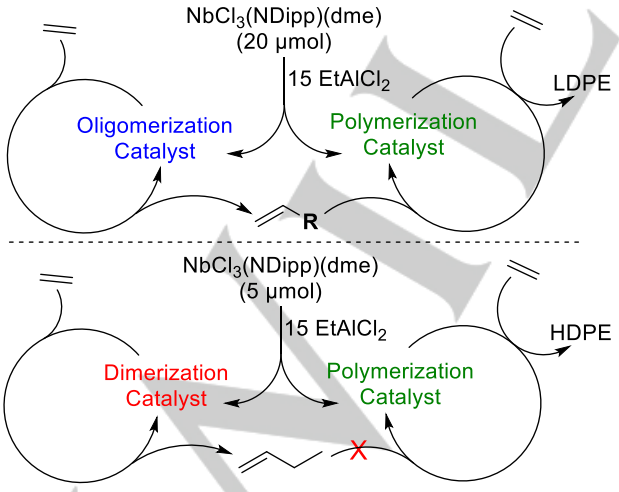

Scheme 2. Proposed concentration-dependent behaviour of pre-catalysts **2d**: at 20 μmol (top) production of LDPE along with oligomers; at 5 μmol (bottom) formation of 1-butene and HDPE.

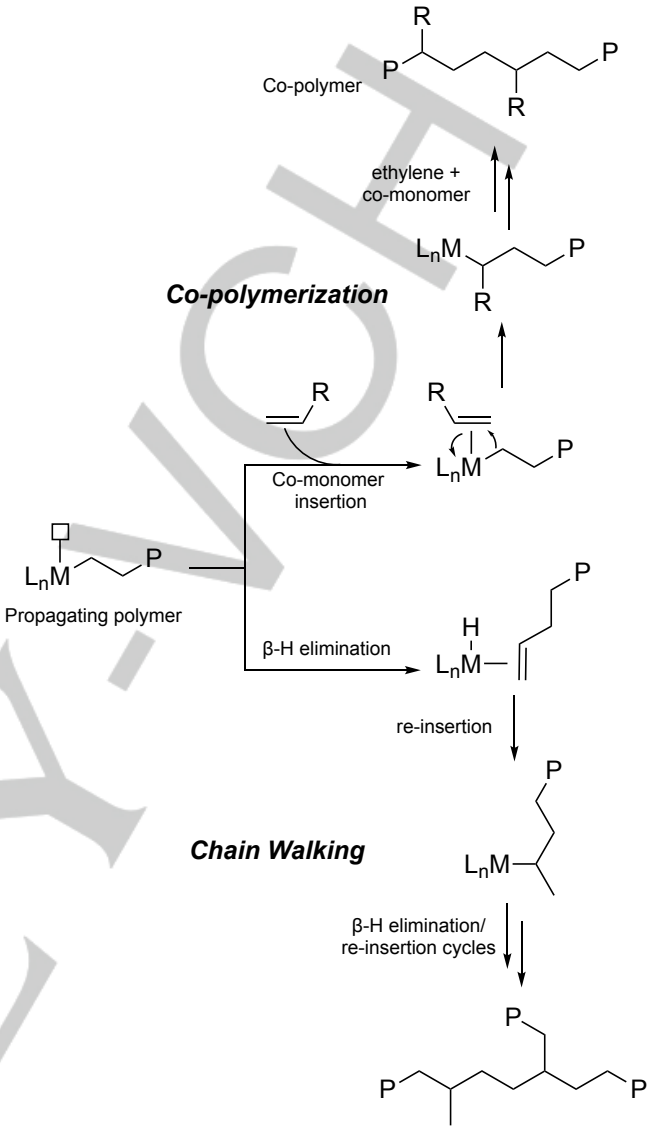

Scheme 3. Comparison of co-polymerization and chain walking pathways for the formation of LDPE.

Ethylene dimerization with tantalum imido complexes

In contrast to the niobium imido pre-catalysts, their corresponding tantalum analogues **3** and **4** performed as dedicated ethylene dimerization systems (Table 2, Runs 7-12) upon activation with 15 equivalents of $EtAlCl_2$. Depending on the imido substituent, activities between 1,786 and 35,709 (mol C_2H_4)(mol Ta)$^{-1}$ h^{-1} were achieved. However, these values are less than half those achieved using the analogous niobium pre-catalysts. This parallels reports in the literature that identify the same trends in relative performance between analogous Nb and Ta polymerization systems.[30b, 35]

The selectivities towards butenes in the liquid fraction achieved using pre-catalysts **3**, **4a-d** in combination with $EtAlCl_2$ were found to be between 77.6 and 80.7 wt%, with low levels of polymer formation (2.2 - 8.8 wt% of the total products fraction).

10.1002/cctc.201801849

However, the most distinctive feature of these tantalum imido systems is their very high selectivity towards butenes, with 1-butene being formed in most cases (Table 2, Runs 7-11); here the predominant by-products are hexenes. This is of key importance considering that 1-butene of high purity is necessary for polymer applications and that separation of C_4 components is costly, whereas separation of C_4 and C_{6+} fractions is comparatively straightforward, hence economically/industrially viable.[12f] Indeed, this type of situation is clearly exemplified by Axens' Alphabutol process where achieving high selectivity rather than high activity is considered more important from an economic standpoint (*vide infra*).

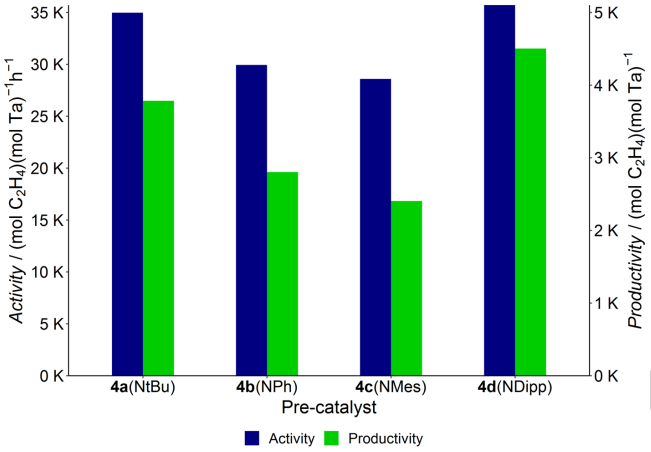

Figure 3. Comparison of catalytic activity and productivity as a function of imido ligand substituent for the tantalum pre-catalysts **4a-d**.

As observed for [CpNbCl$_2$(NDipp)] (**1**) the analogous tantalum complex [CpTaCl$_2$(NDipp)] (**3**) exhibits significantly lower activity and productivity compared to that delivered by its cyclopentadienyl-free counterparts **4a-d** (Table 2). This is attributable to both complexes **1** and **3** having very congested coordination spheres as identified from the topographical steric maps (Table S1). In contrast to the behaviour determined for the niobium-based pre-catalysts **2a-d**, changing the nature of the organoimido ligands of the analogous tantalum systems **4a-d** has a less pronounced effect on catalytic performance.

The catalytic performance of the dme complex (**4d**) versus that of its tmeda (**5**) counterpart were markedly different (Table 2: Run 11 vs Run 12). Although catalysis using pre-catalyst **5** led to a slight decrease in catalytic activity compared with that achieved using **4d**, the productivity increased six-fold with no polymer produced, while the selectivity towards the C_4 and C_6 fractions remained practically unchanged. Unfortunately, the above improvements in catalytic performance derived from the use of tmeda- rather than dme-substituted pre-catalysts came at the cost of selectivity towards 1-butene, which dropped from 100% to 72.4%. This difference in catalytic performance between pre-catalysts **4d** and **5** in combination with EtAlCl$_2$ demonstrate that the Lewis base that stabilizes the tantalum imido complexes (*i.e.* dme and tmeda) can significantly impact catalysis and is not simply displaced from the metal centre and immediately sequestered by the aluminium activator (as observed previously for related molybdenum bis(imido)-derived oligomerization catalysts[10]), hinting at the complexity of the underlying mechanism. However, it should be kept in mind that M-C_{alkyl} bond strengths increase significantly down a group something that will render migratory insertion and reductive elimination processes less favourable for the tantalum systems over the niobium counterparts and hence likely reduce catalytic activity and the preference for polymerisation, consistent with the observed performance (Table 2).[36]

In contrast to the niobium imido pre-catalysts, their tantalum counterparts favour highly selective dimerization. This makes it easier to draw some preliminary conclusions on their mode of operation. When exploring the mechanism of any ethylene oligomerization system the principle pathways to be considered are either a metallacyclic[30a, 37] or a step-wise addition process.[38] From an analysis of the organic products generated by the tantalum imido-based catalysts examined herein (**4a-d**, **5**), the principal dimerization mechanism is consistent with a metallacyclic pathway. Firstly, the complete selectivity of the tantalum imido systems towards 1-butene coupled with the high selectivity towards 1-hexene in the trimer fraction is entirely consistent with a metallacycle mechanism, which is generally considered to be more selective than the alternative step-wise addition pathway.[38, 39] Secondly, the identities of the di- and tri-meric organic products obtained using the tantalum imido pre-catalysts match well with the products that are predicted theoretically to be produced from a metallacyclic pathway rather than those from a step-wise addition process (Table 3). Finally, the synthesis and isolation of tantallacyclopentane derivatives has been reported, something exemplifying their potential formation here under our catalytic test conditions.[40] Nevertheless, it must be noted that a full mechanistic study of this system would be necessary in order to definitively determine the mechanism behind the tantalum imido-mediated dimerization of ethylene, something outside the scope of this preliminary study.[41]

Table 3. Comparison of the expected and experimentally-observed products produced from various oligomerization mechanisms.[a]

	1-C_4	2-C_4	1-C_6	Int. C_6	3 Me-1-C_5	3 Me-2-C_5	2 Et-1-C_4
Step-wise addition with chain walking	✔	✔	✔	✔	✔	✔	✔
Step-wise addition without chain walking	✔		✔	✔			✔
Metallacycle	✔		✔	✔	✔		✔
Observed	✔		✔	✔	✔		✔

[a] See Scheme S1 and S2 for an explanation of how each pathway leads to production of the different products. 1-C_4 = 1-butene, 2-C_4 = 2-butene, 1-C_6 = 1-hexene, Int. C_6 = internal hexenes, 3 Me-1-C_5 = 3 methyl-1-pentene, 3 Me-2-C_5 = 3 methyl-2-pentene, 2 Et-1-C_4 = 2 ethyl-1-butene.

Conclusions

Despite their structural similarity, niobium and tantalum imido pre-catalysts of the type $MCl_3(NR)(dme)$ mediate ethylene oligomerization in strikingly different ways upon activation with $EtAlCl_2$. Although their overall catalytic activity is only moderate, these systems offer unusual product selectivities. Depending on the nature of the organoimido substituent the niobium complexes **2a-d** either instigate dimerization or polymerization of ethylene, with greater steric bulk favouring the latter. Additionally, the nature of the polyethylene produced could be changed from LDPE to HDPE simply by performing the catalysis at a lower niobium concentration. In contrast, the analogous tantalum complexes (**4a-d**, **5**) function as selective ethylene dimerization pre-catalysts with 100% selectivity towards formation of 1-butene, essentially irrespective of the nature of the organoimido substituent, albeit with lower overall activities compared to their niobium counterparts. Lastly, based on the identity of the ethylene dimerization and trimerization products formed, it is concluded that the tantalum imido-mediated ethylene dimerization described herein occurs *via* a metallacyclic rather than a step-wise addition mechanism. Together these results exemplify not only the electronic and steric impact of the organoimido substituent on ethylene oligomerization, which provides a straightforward method of reaction tuning, but also that the catalytic performance of such systems is intimately influenced by the metal, a trend mirrored across both group 5 and 6 systems. Indeed, these results reveal that very subtle changes in pre-catalyst structure can lead to dramatic differences in catalytic performance. Further investigation is intended to further elucidate the specific function of the imido ligands.

Experimental Section

General experimental procedures

All operations were conducted under an atmosphere of dry nitrogen using standard Schlenk and cannula techniques, or in a Saffron Scientific nitrogen-filled glove box, unless otherwise stated. Nitrogen gas was passed through a drying column (silica/$CaCO_3$/P_2O_5). Bulk solvents were purified using an Innovative Technologies SPS facility, except for chlorobenzene, which was dried by distillation from calcium hydride, and for dme that was distilled under nitrogen from sodium/benzophenone. All solvents were degassed prior to use using standard methods. CD_2Cl_2 and CD_3COCD_3 were purchased from Goss Scientific and C_6D_6 from Apollo Scientific. Each deuterated solvent was distilled from CaH_2, degassed and stored under nitrogen. $EtAlCl_2$, $TaCl_5$, $NbCl_3$(dme), and *n*BuLi solution (2.5M in hexanes) were purchased from Sigma-Aldrich and used as received. Bu_3SnCl was purchased from Sigma-Aldrich and degassed prior to use. 2,6-*i*Pr_2-C_6H_3-NH_2 (DippNH_2) and *t*BuNH_2 were purchased from Sigma-Aldrich, distilled from CaH_2 and degassed prior to use. Cyclopentadiene was obtained *via* reactive distillation from dicyclopentadiene, which was purchased from Sigma-Aldrich. $NbCl_5$ and $ZnCl_2$ were purchased from Alfa-Aesar and used as received. Nonane, $MesNH_2$, $PhNH_2$, and pyridine were purchased from Alfa-Aesar, dried over calcium hydride, distilled and degassed prior to use. Solution phase NMR spectra were collected on a Varian Mercury 400 or 200, a Varian Inova 500, a Varian VNMRS-700 or 600 and a Bruker Advance 400 at ambient probe temperatures (290 K) unless otherwise stated. Chemical shifts were referenced to residual proton impurities in the deuterated solvent (^1H), ^{13}C shift of the solvent (^{13}C) or to external 85% H_3PO_4 aqueous solution (^{31}P).[42] ^1H and ^{13}C NMR spectra were assigned with the aid of COSY, HSQC and HMBC experiments. Chemical shifts are reported in ppm and coupling constants in Hz. GC-FID analyses were conducted on a Perkin Elmer Clarus 400 GC or an Agilent Technologies 6890N GC instrument, both equipped with a PONA column (50 m × 0.20 mm × 0.50 µm) and supplied with H_2 as a carrier gas. Hydrogenative GC-FID analysis was performed using an Agilent Technologies 6890N or a Perkin Elmer Clarus 400 GC System equipped with an inlet liner packed with hydrogenating catalyst (Pt on Chromosorb W at 200 ºC) and PONA column (50 m × 0.20 mm × 0.50 μm).[43] DSC analysis of polyethylene was performed on a TA Instruments DSC Q1000. The samples were heated from room temperature to 200 °C with a heating rate of 10 °C/min. The temperature of each sample was held constant at 200 °C for five minutes in order to erase its thermal history and then cooled down to 10 °C with a cooling rate of 10 °C/min. The samples were then kept at 10 °C for five minutes followed by re-heating at 10 °C/min to 200 °C. The peak melting temperature and the crystallinity were determined from the final heating cycle,[30a] while the density of each resin was calculated from the peak melting temperature according to literature procedures.[44] Traditional GPC analysis of the polyethylene samples was not possible since samples were either insoluble or, at best, only partially soluble in 1,2-dichlorobenzene or in 1,1,2,2-tetrachloroethane (even at 150 °C). Catalysis experiments were performed in a batch fashion in 250 mL volume Buchi Miniclaves or in a 1.2 L volume Premex Pinto autoclave equipped with stainless steel vessels with integral thermal-fluid jackets (connected to a Huber 405 W thermostatic bath), internal cooling coils (tap water), and mechanical mixing *via* customized gas-entraining stirrers (1000 rpm). Dried and degassed solvent was added *via* a gas-tight syringe under Ar (Grade 4.5, supplied by Linde). Ethylene (Grade 4.5) was supplied by Linde and passed through oxygen and moisture scrubbing columns prior to use; ethylene flow was measured using a Siemens Sitrans F C Massflo system (Mass 6000-Mass 2100) and the data logged. All catalytic tests were allowed to run until ethylene uptake had dropped below 0.2 g min^{-1} or the reactor had become filled with product.

Synthesis of reagents and complexes

The following compounds were all prepared according to previously reported literature procedures or slight modifications thereof: [CpSn*n*Bu_3],[45] DippNHTMS,[46] [$CpNbCl_4$],[47] [$CpNbCl_2$(NDipp)] (**1**),[16d] [$NbCl_3$(N*t*Bu)(dme)] (**2a**),[16a] [$NbCl_3$(NPh)(dme)] (**2b**),[16a] [$NbCl_3$(NDipp)(dme)] (**2d**),[16a] [$CpTaCl_4$],[47] [$CpTaCl_2$(NDipp)] (**3**),[16b] [$TaCl_3$(N*t*Bu)(dme)] (**4a**),[16a] [$TaCl_3$(NPh)(dme)] (**4b**),[16a] [$TaCl_3$(NDipp)(dme)] (**4d**),[16a] and [$TaCl_3$(NDipp)(tmeda)] (**5**).[16c] Successful synthesis was confirmed by comparison of the ^1H and ^{13}C NMR spectra of the obtained product with the spectra reported in the literature.

[$NbCl_3$(NMes)(dme)] (2c). An adaptation of the method described by Korolev *et al.* was used:[16a] a Schlenk was loaded with $NbCl_5$ (5.00 g, 18.5 mmol) and 1,2-dimethoxyethane (3.30 mL), with the resulting mixture being stirred until the solids dissolved. $ZnCl_2$ (5.02 g, 36.8 mmol) was added to the solution to give a white precipitate. The mixture was then cooled to –40 °C and a solution of $MesNH_2$ (2.60 mL, 18.5 mmol) and pyridine (2.98 mL, 36.8 mmol) in CH_2Cl_2 (20 mL) was added drop-wise. After addition was complete, the white precipitate dissolved and the dark purple solution generated was stirred at ambient temperature. After 17 hours of stirring a white precipitate formed, which was removed by filtration. The filtrate was evaporated to dryness to give a purple solid, which was extracted with hot CH_2Cl_2 until the extracts were lightly coloured. The extracts were combined, condensed, and stored at –35 °C. After 17 hours purple crystals formed, which were isolated, ground and dried under reduced pressure to give **2c** in the form of a purple powder in 63% yield (4.93 g). Crystals of **2c** suitable for an X-ray crystallographic analysis were

obtained by layering a DCM solution of the compound with pentane. ^{1}H NMR (700 MHz, $CDCl_3$) δ = 6.76 (s, 2H, H_m), 4.14 (m, 2H, OCH_{2A}), 4.08(m, 2H, OCH_{2B}), 3.98 (s, 3H, OCH_{3A}), 3.95 (s, 3H, OCH_{3B}), 2.79 (s, 6H, C_oCH_3), 2.30 (s, 3H, C_pCH_3); ^{13}C NMR (176 MHz, $CDCl_3$) δ = 151.15 (s, C_{ipso}), 138.21 (s, C_o), 137.04 (s, C_p), 128.15 (s, C_m), 75.67 (s, OCH_{2A}), 70.77 (s, OCH_{2B}), 69.06 (s, OCH_{3A}), 62.53 (s, OCH_{3B}), 21.10 (s, C_pCH_3), 19.36 (s, C_oCH_3); elemental analysis calcd (%) for $C_{13}H_{21}Cl_3NNbO_2$ (422.57): C 36.95, H 5.01, N 3.31; found: C 37.05, H 4.89, N 3.33.

[$TaCl_3$(NMes)(dme)] (4c). This complex was synthesized according to a modification of the procedure described for [$NbCl_3$(NMes)(dme)] (**2c**) using $TaCl_5$ (5.00 g, 14.0 mmol), $ZnCl_2$ (3.80 g, 27.9 mmol), $MesNH_2$ (1.97 mL, 14.0 mmol), pyridine (2.26 mL, 27.9 mmol), and CH_2Cl_2 (20 mL) to give **4c** as a yellow powder in 72% yield (5.13 g). Crystals of **4c** suitable for an X-ray crystallographic analysis were obtained by layering a concentrated DCM solution of the complex with pentane. ^{1}H NMR (700 MHz, $CDCl_3$) δ = 6.85 (s, 2H, H_m), 4.22 (m, 2H, OCH_{2A}), 4.12 (s, 3H, OCH_{3A}), 4.08 (m, 2H, OCH_{2B}), 4.01 (s, 3H, OCH_{3B}), 2.79 (s, 6H, C_oCH_3), 2.40 (s, 3H, C_pCH_3); ^{13}C NMR (176 MHz, $CDCl_3$) δ = 148.85 (s, C_{ipso}), 138.52 (s, C_o), 135.45 (s, C_p), 127.51 (s, C_m), 76.12 (s, OCH_{2A}), 71.00 (s, OCH_{3A}), 70.31 (s, OCH_{2A}), 63.00 (s, OCH_{3B}), 20.71 (s, C_pCH_3), 19.14 (s, C_oCH_3); elemental analysis calcd (%) for $C_{13}H_{21}Cl_3NTaO_2$ (510.61): C 30.58, H 4.15, N 2.74; found: C 30.61, H 4.09, N 2.77.

Catalytic ethylene dimerization test protocol

Dilute stock solutions (PhCl) of each of the pre-catalysts were prepared and stored in glass ampoules fitted with J Youngs' taps using standard Schlenk techniques. The rigorously cleaned autoclave was heated (130 °C) under vacuum for 60 mins, then cooled to reaction temperature (60 °C) and back-filled with ethylene (10 barg), which was then vented to 0 barg *via* a septum to purge the inlet valve. Dried and degassed solvent (PhCl, 74 mL) and pre-catalyst stock solution (4.00 mL, 20 µmol) were then added sequentially *via* syringe. The autoclave was pressurized with ethylene to 10 barg and vented. The appropriate quantity (0.60 mL, 300 µmol) of a stock solution of the activator $EtAlCl_2$ (0.50 M in PhCl) was added to initiate catalysis and the vessel was immediately pressurised with ethylene (40 barg). The pressure was kept constant throughout the reaction by the continuous addition of ethylene, which was controlled and monitored *via* the flow meter. Heating and cooling were controlled to maintain a stable reaction temperature. Once ethylene uptake had dropped below 0.2 g min^{-1}, or the autoclave was filled by product, the gas supply was closed and the reactor was cooled to and maintained at 5 °C or lower using an ice bath. The reactor was then slowly and carefully vented with a portion of the vent gas being directly fed to a GC-FID instrument equipped with gas-sampling loop; where butenes were observed here by GC, the amount lost was ≤5% of the total butenes content of the liquid fraction. The reactor contents were treated with 1000 µL of nonane (GC internal standard) and 10% HCl (aq) and a sample of the cold reaction mixture was collected with a cold (–30 °C) pipette and extracted into cold (-30 °C) toluene. A sample of the organic phase was immediately taken for GC-FID analysis as well as hydrogenative GC-FID analysis for determination of the branching selectivity in the trimers fraction. Any precipitated polyethylene formed was collected by filtration, washed first with 10% HCl (aq) and then repeatedly with EtOH to remove all metal-containing salts, then finally washed with acetone before drying to constant weight overnight at 100 °C and weighed.

Acknowledgements

The authors thank Sasol Group Technology, the EPSRC, and Durham University for funding and permission to publish this work. Dr David Smith (Sasol Group Technology) and Mr Douglas Carswell (Durham University) are thanked for fruitful discussions and for performing the DSC analyses, respectively.

Keywords: dimerization • ethylene • niobium • tantalum • imido

[1] a) J. C. Mol, *J. Mol. Catal. A: Chem.* **2004**, *213*, 39-45; b) W. Kaminsky, M. Arndt-Rosenau, in *Applied Homogeneous Catalysis with Organometallic Compounds*, Wiley-VCH Verlag GmbH, **2008**, pp. 213-385; c) C. Bergemann, R. Cropp, G. Luft, *J. Mol. Catal. A: Chem.* **1996**, *105*, 87-91; d) M. Morgan, *IHS Chemical Bulletin* **2016**, *2*, 3-6.

[2] a) G. S. Lee, J. H. McCain, M. M. Bhasin, *Kent and Riegel's Handbook of Industrial Chemistry and Biotechnology*, Springer Science & Business Media, Boston, MA, **2007**; b) P.-A. R. Breuil, L. Magna, H. Olivier-Bourbigou, *Catal. Lett.* **2015**, *145*, 173-192.

[3] F. M. Geilen, G. Stochniol, S. Peitz, E. Schulte-Koerne, *Ullmann's Encyclopedia of Industrial Chemistry* **2014**.

[4] a) H. Zhang, X. Li, Y. Zhang, S. Lin, G. Li, L. Chen, Y. Fang, H. Xin, X. Li, *Energy Environ. Focus* **2014**, *3*, 246-256; b) A. Finiels, F. Fajula, V. Hulea, *Cat. Sci. Technol.* **2014**, *4*, 2412-2426; c) M. J. Lamb, D. C. Apperley, M. J. Watson, P. W. Dyer, *Top. Catal.* **2018**, *61*, 213-224; d) R. G. Schultz, *J. Catal.* **1967**, *7*, 286-290; e) Z. Xu, J. P. Chada, L. Xu, D. Zhao, D. C. Rosenfeld, J. L. Rogers, I. Hermans, M. Mavrikakis, G. W. Huber, *ACS Catal.* **2018**, *8*, 2488-2497.

[5] a) N. Ajellal, M. C. A. Kuhn, A. D. G. Boff, M. Hörner, C. M. Thomas, J.-F. Carpentier, O. L. Casagrande, *Organometallics* **2006**, *25*, 1213-1216; b) A. Ulbrich, R. R. Campedelli, J. L. S. Milani, J. H. Z. dos Santos, O. D. Casagrande, *Appl. Catal., A* **2013**, *453*, 280-286; c) S. Murtuza, O. L. Casagrande, R. F. Jordan, *Organometallics* **2002**, *21*, 1882-1890; d) M. P. Gil, J. H. Z. dos Santos, O. L. Casagrande, *Macromol. Chem. Phys.* **2001**, *202*, 319-324; e) L. G. Furlan, M. P. Gil, O. L. Casagrande, *Macromol. Rapid Commun.* **2000**, *21*, 1054-1057.

[6] a) S. J. Song, Y. Li, C. Redshaw, F. S. Wang, W. H. Sun, *J. Organomet. Chem.* **2011**, *696*, 3772-3778; b) T. Xiao, J. Lai, S. Zhang, X. Hao, W.-H. Sun, *Cat. Sci. Technol.* **2011**, *1*, 462-469.

[7] a) C. T. Burns, R. F. Jordan, *Organometallics* **2007**, *26*, 6726-6736; b) V. Khlebnikov, A. Meduri, H. Mueller-Bunz, T. Montini, P. Fornasiero, E. Zangrando, B. Milani, M. Albrecht, *Organometallics* **2012**, *31*, 976-986.

[8] a) Y. Sheng, Z. Y. Geng, Y. C. Wang, Y. Z. Wang, X. J. Sun, *Chin. J. Chem.* **2011**, *29*, 1084-1094; b) M. Shiotsuki, P. S. White, M. Brookhart, J. L. Templeton, *J. Am. Chem. Soc.* **2007**, *129*, 4058-4067.

[9] P. R. Elowe, C. McCann, P. G. Pringle, S. K. Spitzmesser, J. E. Bercaw, *Organometallics* **2006**, *25*, 5255-5260.

[10] W. R. H. Wright, A. S. Batsanov, A. M. Messinis, J. A. K. Howard, R. P. Tooze, M. J. Hanton, P. W. Dyer, *Dalton Trans.* **2012**, *41*, 5502-5511.

[11] a) S. Zhang, K. Nomura, *J. Am. Chem. Soc.* **2010**, *132*, 4960-4965; b) A. Igarashi, S. Zhang, K. Nomura, *Organometallics* **2012**, *31*, 3575-3581; c) K. Nomura, A. Igarashi, S. Katao, W. J. Zhang, W. H. Sun, *Inorg. Chem.* **2013**, *52*, 2607-2614; d) X.-Y. Tang, A. Igarashi, W.-H. Sun, A. Inagaki, J. Liu, W. Zhang, Y.-S. Li, K. Nomura, *Organometallics* **2014**, *33*, 1053-1060.

[12] a) F. Grasset, L. Magna (IFP Energies Nouvelles), US8,624,042_B2, **2014**; b) H. Olivier, P. Laurent-Gerot, *J. Mol. Catal. A: Chem.* **1999**, *148*, 43-48; c) L. Magna, H. Olivier-Bourbigou (IFP Energies Nouvelles), US9,499,455_B2, **2016**; d) N. Le Quan, D. Cruypelinck, D. Commereur, Y. Chauvin, G. Leger (IFP Energies Nouvelles), EP0,135,441 B1, **1985**; e) V. I. Zhukov, N. P. Shestak, G. P. Belov, M. N. Dyadjunova, L. A. Shilov, I. D. Shevlyakov, F. S. Dyachkovsky, A. G. Liakumovich, P. A. Vernov US4,101,600, **1978**; f) A. Forestiere, H. Olivier-Bourbigou, L. Saussine, *Oil Gas Sci. Technol.* **2009**, *64*, 649-667; g) A. W. Al-Sa'doun, *App. Cat. A: General* **1993**, *105*, 1-40; h) J. B. Cazaux, P. Braunstein, L. Magna, L. Saussine, H. Olivier-Bourbigou, *Eur. J. Inorg. Chem.* **2009**, 2942-2950; i) I. Ono, S. Yamada, H. Abe, K. Tago, N. Kunihiro US3,686,350, **1972**; j) G. P. Belov, T. S. Dzhabiev, F. S. Dyachkovsky, V. I. Smirnov, N. D. Karpova, K.-M. A. Brikenshtein, M. P. Gerasina, V.

E. Kuzmin, P. E. Matkovsky, L. N. Russiyan, A. D. Pomogalio, N. M. Chirkov US3,879,485, **1975**.

[13] H. G. Alt, *Polyolefins Journal* **2015**, *2*, 17-25.

[14] a) A. M. Messinis, A. S. Batsanov, W. R. H. Wright, J. A. K. Howard, M. J. Hanton, P. W. Dyer, *ACS Catal.* **2018**, *8*, 11249-11263; b) A. M. Messinis, W. R. H. Wright, A. S. Batsanov, J. A. K. Howard, M. J. Hanton, P. W. Dyer, *ACS Catal.* **2018**, *8*, 11235-11248.

[15] a) J. D. Fellmann, G. A. Rupprecht, R. R. Schrock, *J. Am. Chem. Soc.* **1979**, *101*, 5099-5101; b) B. H. Chang, C. P. Lau, R. H. Grubbs, C. H. Brubaker, *J. Organomet. Chem.* **1985**, *281*, 213-220; c) M. Taoufik, A. de Mallmann, E. Prouzet, G. Saggio, J. Thivolle-Cazat, J. M. Basset, *Organometallics* **2001**, *20*, 5518-5521; d) R. R. Schrock (Massachusetts Institute of Technology), US 4,245,131, **1981**; e) R. R. Schrock, R. A. Dubois (The Dow Chemical Company), US 0 282 630 B1, **1987**; f) V. C. Gibson, T. P. Kee, A. D. Poole, *J. Chem. Soc., Chem. Commun.* **1990**, 1720-1722.

[16] a) A. V. Korolev, A. L. Rheingold, D. S. Williams, *Inorg. Chem.* **1997**, *36*, 2647-2655; b) G. L. Nikonov, P. Mountford, S. K. Ignatov, J. C. Green, M. A. Leech, L. G. Kuzmina, A. G. Razuvaev, N. H. Rees, A. J. Blake, J. A. K. Howard, D. A. Lemenovskii, *J. Chem. Soc., Dalton Trans.* **2001**, 2903-2915; c) K. S. Heinselman, V. M. Miskowski, S. J. Geib, L. C. Wang, M. D. Hopkins, *Inorg. Chem.* **1997**, *36*, 5530-5538; d) D. N. Williams, J. P. Mitchell, A. D. Poole, U. Siemeling, W. Clegg, D. C. R. Hockless, P. A. Oneil, V. C. Gibson, *J. Chem. Soc., Dalton Trans.* **1992**, 739-751; e) M. Gómez, C. Hernández-Prieto, A. Martín, M. Mena, C. Santamaría, *Inorg. Chem.* **2017**, *56*, 11681-11687.

[17] a) D. E. Wigley, *Organoimido Complexes of the Transition Metals*, John Wiley & Sons, Inc., **2007**; b) W. A. Nugent, R. L. Harlow, *J. Am. Chem. Soc.* **1994**, *116*, 6142-6148.

[18] a) L. Falivene, R. Credendino, A. Poater, A. Petta, L. Serra, R. Oliva, V. Scarano, L. Cavallo, *Organometallics* **2016**, *35*, 2286-2293; b) A. Poater, B. Cosenza, A. Correa, S. Giudice, F. Ragone, V. Scarano, L. Cavallo, *Eur. J. Inorg. Chem.* **2009**, *2009*, 1759-1766; c) A. Poater, F. Ragone, S. Giudice, C. Costabile, R. Dorta, S. P. Nolan, L. Cavallo, *Organometallics* **2008**, *27*, 2679-2681; d) A. Poater, F. Ragone, R. Mariz, R. Dorta, L. Cavallo, *Chem. Eur. J.* **2010**, *16*, 14348-14353.

[19] https://www.molnac.unisa.it/OMtools/sambvca2.0/

[20] a) P. D. Lyne, D. M. P. Mingos, *J. Organomet. Chem.* **1994**, *478*, 141-151; b) A. Pidcock, R. E. Richards, L. M. Venanzi, *J. Chem. Soc. A: Inorg., Phys., Theor.* **1966**, 1707-1710; c) F. Basolo, R. G. Pearson, in *Prog. Inorg. Chem., Vol. 4*, **1962**, pp. 381-453; d) G. R. Clark, A. J. Nielson, C. E. F. Rickard, *J. Chem. Soc., Dalton Trans.* **1995**, 1907-1914.

[21] J. G. Speight, *Lange's Handbook of Chemistry*, Sixteenth Edition ed., McGraw-Hill, **2005**.

[22] N. Kaltsoyannis, P. Mountford, *J. Chem. Soc., Dalton Trans.* **1999**, 781-790.

[23] For note, previously Williams and colleagues sought to explore the electronic characteristics of a number of the niobium (**2**) and tantalum (**4**) imido complexes through examination of the M-N vibrational bands by IR spectroscopy.[16a]. However, there is no single mode that is solely M-N in character, rather the M-N components are strongly coupled to N-C and C-H or C-C modes in these imido complexes. This is in agreement with a prior study, which also tried to assess the electronic characteristics of imido complexes using Raman spectroscopy. See: W. P. Griffith, A. J. Nielson, M. J. Taylor, *J. Chem. Soc. Dalton Trans.* **1988**, 647–649.

[24] M. J. Hanton, L. Daubney, T. Lebl, S. Polas, D. M. Smith, A. Willemse, *Dalton Trans.* **2010**, *39*, 7025-7037.

[25] E. Y.-X. Chen, T. J. Marks, *Chem. Rev.* **2000**, *100*, 1391-1434.

[26] M. P. Coles, C. I. Dalby, V. C. Gibson, I. R. Little, E. L. Marshall, M. H. R. da Costa, S. Mastroianni, *J. Organomet. Chem.* **1999**, *591*, 78-87.

[27] A. M. R. Galletti, G. Pampaloni, *Coord. Chem. Rev.* **2010**, *254*, 525-536.

[28] R. Walsh, D. H. Morgan, A. Bollmann, J. T. Dixon, *App. Cat. A: General* **2006**, *306*, 184-191.

[29] a) F. Marchetti, G. Pampaloni, Y. Patil, A. M. R. Galletti, M. Hayatifar, *Polym. Int.* **2011**, *60*, 1722-1727; b) F. Marchetti, G. Pampaloni, Y. Patil, A. M. R. Galletti, F. Renili, S. Zacchini, *Organometallics* **2011**, *30*, 1682-1688; c) F. Marchetti, G. Pampaloni, Y. Patil, A. Maria, R. Galletti, S. Zacchini, *J. Polym. Sci. Part a-Polymer Chemistry* **2011**, *49*, 1664-1670.

[30] a) Y. Chen, R. Credendino, E. Callens, M. Atiqullah, M. A. Al-Harthi, L. Cavallo, J.-M. Basset, *ACS Catal.* **2013**, 1360-1364; b) C. Redshaw, M. Rowan, D. M. Homden, M. R. L. Elsegood, T. Yamato, C. Perez-Casas, *Chem. Eur. J.* **2007**, *13*, 10129-10139; c) L. Contat-Rodrigo, A. Ribes-Greus, C. T. Imrie, *J. Appl. Polym. Sci.* **2002**, *86*, 764-772.

[31] a) C. A. Fonseca, I. R. Harrison, *Thermochim. Acta* **1998**, *313*, 37-41; b) Y. Gelfer, H. H. Winter, *Macromolecules* **1999**, *32*, 8974-8981.

[32] a) B. Zhu, C. Guo, Z. Liu, Y. Yin, *J. Appl. Polym. Sci.* **2004**, *94*, 2451-2455; b) Z. J. A. Komon, X. Bu, G. C. Bazan, *J. Am. Chem. Soc.* **2000**, *122*, 1830-1831; c) Z. J. A. Komon, G. M. Diamond, M. K. Leclerc, V. Murphy, M. Okazaki, G. C. Bazan, *J. Am. Chem. Soc.* **2002**, *124*, 15280-15285; d) M. Frediani, C. Piel, W. Kaminsky, C. Bianchini, L. Rosi, *Macromolecular Symposia* **2006**, *236*, 124-133; e) S. Guo, H. Fan, Z. Bu, B.-G. Li, S. Zhu, *Macromol. React. Eng.* **2015**, *9*, 32-39.

[33] a) L. Guo, S. Dai, X. Sui, C. Chen, *ACS Catal.*, **2016**, *6*, 428–441; b) C. Chen, *Nat. Rev. Chem.*, **2018**, *2*, 6–14; c) L. Guo, W. Liu, C. Chen, *Mater. Chem. Front.*, **2017**, *1*, 2487–2494; d) K. S. O'Connor, J. R. Lamb, T. Vaidya, I. Keresztes, K. Klimovica, A. M. LaPointe, O. Daugulis, G. W. Coates, *Macromolecules*, **2017**, *50*, 7010–7027.

[34] S. Murtuza, S. B. Harkins, G. S. Long and A. Sen, *J. Am. Chem. Soc.*, **2000**, *122*, 1867–1872.

[35] K. Mashima, S. Fujikawa, Y. Tanaka, H. Urata, T. Oshiki, E. Tanaka, A. Nakamura, *Organometallics* **1995**, *14*, 2633-2640.

[36] a) P. E. M. Siegbahn, *J. Phys. Chem.* **1995**, *99*, 12723-12729; b) M. Brookhart, E. Hauptman, D. M. Lincoln, *J. Am. Chem. Soc.* **1992**, *114*, 10394-10401.

[37] a) A. K. Tomov, J. J. Chirinos, D. J. Jones, R. J. Long, V. C. Gibson, *J. Am. Chem. Soc.* **2005**, *127*, 10166-10167; b) A. K. Tomov, J. J. Chirinos, R. J. Long, V. C. Gibson, M. R. J. Elsegood, *J. Am. Chem. Soc.* **2006**, *128*, 7704-7705; c) J. T. Dixon, M. J. Green, F. M. Hess, D. H. Morgan, *J. Organomet. Chem.* **2004**, *689*, 3641-3668; d) D. S. McGuinness, *Organometallics* **2009**, *28*, 244-248; e) Y. Qi, Q. Dong, L. Zhong, Z. Liu, P. Qiu, R. Cheng, X. He, J. Vanderbilt, B. Liu, *Organometallics* **2010**, *29*, 1588-1602; f) Z. X. Yu, K. N. Houk, *Angew. Chem.-Int. Ed.* **2003**, *42*, 808-811.

[38] a) S. M. Pillai, M. Ravindranathan, S. Sivaram, *Chem. Rev.* **1986**, *86*, 353-399; b) S. D. Ittel, L. K. Johnson, M. Brookhart, *Chem. Rev.* **2000**, *100*, 1169-1203; c) J. Skupinska, *Chem. Rev.* **1991**, *91*, 613-648; d) O. Novaro, S. Chow, P. Magnouat, *J. Catal.* **1976**, *41*, 91-100.

[39] D. S. McGuinness, *Chem. Rev.* **2011**, *111*, 2321-2341.

[40] J. M. Mayer and J. E. Bercaw, *J. Am. Chem. Soc.*, **1982**, *104*, 2157–2165.

[41] J. A. Suttil, D. S. McGuinness, *Organometallics* **2012**, *31*, 7004-7010.

[42] G. R. Fulmer, A. J. M. Miller, N. H. Sherden, H. E. Gottlieb, A. Nudelman, B. M. Stoltz, J. E. Bercaw, K. I. Goldberg, *Organometallics* **2010**, *29*, 2176-2179.

[43] T. E. Kuzmenko, A. L. Samusenko, V. P. Uralets, R. V. Golovnya, *J. High. Resolut. Chromatogr.* **1979**, *2*, 43-44.

[44] C. K. Chai, C. J. Frye (BP Chemicals Limited), US 6,642,339 B1, **2003**.

[45] A. C. Reddy, E. D. Jemmis, O. J. Scherer, R. Winter, G. Heckmann, G. Wolmershauser, *Organometallics* **1992**, *11*, 3894-3900.

[46] V. Chandrasekhar, R. Boomishankar, R. Azhakar, K. Gopal, A. Steiner, S. Zacchini, *Eur. J. Inorg. Chem.* **2005**, 1880-1885.

[47] M. J. Bunker, A. Decian, M. L. H. Green, J. J. E. Moreau, N. Siganporia, *J. Chem. Soc., Dalton Trans.* **1980**, 2155-2161.

10.1002/cctc.201801849

WILEY-VCH

Entry for the Table of Contents

FULL PAPER

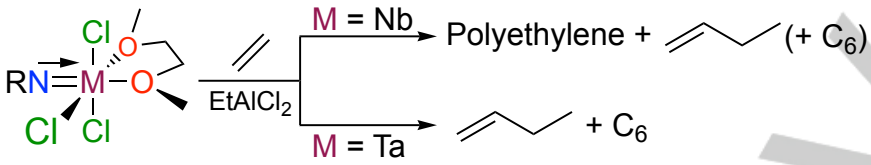

Tuning catalysis: Activation of niobium mono(imido) complexes with $EtAlCl_2$ affords catalysts that produce dimers or polyethylene depending on the nature of the imido substituent. In contrast, the analogous tantalum systems, irrespective of the organoimido motif, mediate predominantly ethylene di- and tri-merization with overall selectivities to butenes of between 73.0 - 80.7 wt% and selectivity within the dimer fraction to 1-butene in the range 72.4 to 100%.

A. M. Messinis, A. S. Batsanov, J. A. K. Howard, M. J. Hanton, P. W. Dyer**

Page No. – Page No.

Activated niobium and tantalum imido complexes: from tuneable polymerization to selective ethylene dimerization systems